Radial Acceleration Relation in Rotationally Supported Galaxies

Stacy S. McGaugh, Federico Lelli, and James M. Schombert

The Radial Acceleration Relation in Rotationally Supported Galaxies

Stacy S. McGaugh and Federico Lelli
Department of Astronomy, Case Western Reserve University,
10900 Euclid Avenue, Cleveland, OH 44106, USA

James M. Schombert
Department of Physics, University of Oregon, Eugene, OR 97403, USA

We report a correlation between the radial acceleration traced by rotation curves and that predicted by the observed distribution of baryons. The same relation is followed by 2693 points in 153 galaxies with very different morphologies, masses, sizes, and gas fractions. The correlation persists even when dark matter dominates. Consequently, the dark matter contribution is fully specified by that of the baryons. The observed scatter is small and largely dominated by observational uncertainties. This radial acceleration relation is tantamount to a natural law for rotating galaxies.

INTRODUCTION

The missing mass problem in extragalactic systems is well established. The observed gravitational potential cannot be explained by the stars and gas. A classic example is that the rotation curves of disk galaxies become approximately flat ($V \approx$ constant) when they should be falling in a Keplerian ($V \propto R^{-1/2}$) fashion [1, 2].

The flatness of rotation curves is only the beginning of the story of the mass discrepancy in galaxies. For example, the baryonic mass of a galaxy (the sum of its stars and gas: $M_{\mathrm{bar}} = M_\star + M_g$) correlates with the amplitude of the flat rotation velocity V_f. This baryonic Tully-Fisher relation [3–5] is a simple scaling relation ($M_{\mathrm{bar}} \propto V_f^4$) with no apparent dependence on other properties like galaxy size [6, 7] or surface brightness [8, 9]. It has remarkably little intrinsic scatter [10–12]. This implies a strong connection between the baryons and the physics that sets V_f.

There are further indications on a connection between baryons and dynamics. Features like spiral arms have corresponding bumps in rotation curve [13]. The ratio of dark to baryonic mass is known to depend on acceleration [14, 15]. Here we demonstrate the existence of a quantitative relation between the acceleration due to the baryons and that due to the total mass. A key advance is that near-infrared photometry provides a direct link between starlight and stellar mass: the relation follows from the data with no adjustable parameters.

DATA

Galaxies come in a wide range of morphologies, masses, sizes, and densities. Generically they are either pressure supported (ellipticals) or rotationally supported (spirals and irregulars). Here we consider rotationally supported systems where the rotation curve provides a direct tracer of the centripetal acceleration:

$$\mathrm{g_{obs}} = \frac{V^2(R)}{R} = \left| \frac{\partial \Phi_{\mathrm{tot}}}{\partial R} \right|, \qquad (1)$$

where Φ_{tot} is the gravitational potential and $V(R)$ is the full, resolved rotation curve. We do not consider pressure supported elliptical galaxies for which the derivation of the potential is more complex, but there are indications that they may obey a similar phenomenology [16–18].

Galaxy Sample

We employ the new Spitzer Photometry and Accurate Rotation Curves (SPARC) database [19]. SPARC is a sample of 175 disk galaxies representing all rotationally supported morphological types. It includes near-infrared (3.6μm) observations that trace the distribution of stellar mass and 21 cm observations that trace the atomic gas. The 21 cm data also provide velocity fields from which the rotation curves are derived. In some cases these are supplemented by high spatial resolution observations of ionized interstellar gas. SPARC is the largest galaxy sample to date with spatially resolved data on the distribution of both stars and gas as well as rotation curves for every galaxy. See [19] for a complete description of the sample and associated data.

For the purposes of this study, we apply a few modest quality criteria. Ten face-on galaxies with $i < 30°$ are rejected to minimize $\sin(i)$ corrections to the observed velocities. Twelve galaxies with asymmetric rotation curves that manifestly do not trace the equilibrium gravitational potential are rejected. This leaves a sample of 153 galaxies. Of the many resolved points along the rotation curves of these galaxies, we require a minimum precision of 10% in velocity. This retains 2693 data points out of 3149. Dropping this last requirement has no affect on the result; it merely increases the scatter as expected for less accurate data.

SPARC extends over an exceptional range of physical properties (Fig. 1). It includes galaxies with rotation
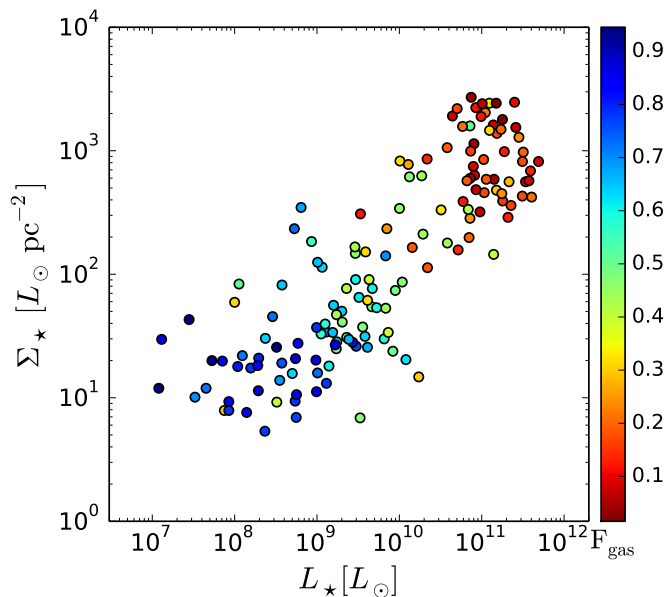
FIG. 1. The distribution of SPARC galaxies in luminosity and effective surface brightness. Points are coded by gas fraction (side bar). SPARC samples all known properties of rotationally supported galaxies, from low to high mass, low to high surface brightness, and negligible to dominant gas content.

velocities $20 < V_f < 300$ km s^{-1}, luminosities $10^7 < L_{[3.6]} < 5 \times 10^{11}$ L$_\odot$, gas masses $10^7 < M_{gas} < 5 \times 10^{10}$ M$_\odot$, gas fractions $0.01 < F_{gas} < 0.97$, half-light radii $0.3 < R_{1/2} < 5$ kpc, and effective surface brightnesses $5 < \Sigma_\star < 3 \times 10^3$ L$_\odot$ pc^{-2}. This range extends from some of largest individual galaxies known to many of the smallest. SPARC samples well the range of properties of disk galaxies found in complete samples [20–22]. Low mass and low surface brightness galaxies are particularly well represented in SPARC, in contrast to flux selected samples that are typically restricted to $M_\star > 10^9$ M$_\odot$ and $V_f > 100$ km s^{-1}.

All galaxies have been observed [23] at 3.6 μm with the *Spitzer Space Telescope*. This provides the most accurate available tracer of the stellar mass [24–26]. Critically, there is little variation in the conversion from starlight to stellar mass [11, 27]: what you see in the near-infrared is what you get for the gravitational potential of the stars. We have uniformly analyzed all of the photometric data using the procedures described in [23].

Galaxies were selected for the availability of resolved 21 cm data. These interferometric data are expensive in both telescope time and labor, and are the limiting factor on sample size. These rotation curves represent the fruits of decades of work by an entire community of radio astronomers (see references in [19]). SPARC provides the broadest view of disk galaxies currently available.

The Gravitational Potentials of Baryons

Baryonic mass models are constructed from the observed distribution of stars and gas. Azimuthally averaged surface brightness profiles are converted to surface density assuming a constant mass-to-light ratio for the stars. The same prescription is used in all galaxies (see below). The conversion for gas is known from the physics of the spin-flip transition of atomic hydrogen [28]. The atomic gas profiles are scaled up by a factor of 1.33 to account for the cosmic abundance of helium [29]. We make the customary assumption that galactic disks have a small but finite thickness to obtain the 3D density ρ_{bar} [19]. While it is important to account for the cylindrical rather than spherical geometry of disks [30, 31], the results are not sensitive to the detailed implementation of disk thickness.

We solve the Poisson equation

$$\nabla^2 \Phi_{bar} = 4\pi G \rho_{bar} \tag{2}$$

numerically [30–32] to determine the gravitational potential Φ_{bar} of each baryonic component (Fig. 2). The acceleration due to the sum of baryonic components is

$$g_{bar} = \left| \frac{\partial \Phi_{bar}}{\partial R} \right| . \tag{3}$$

Note that this refers only to the observed baryons. It is measured independently of the actual acceleration g_{obs} obtained from the rotation curve.

While the majority of stars and gas resides in thin disks, some galaxies have a central, quasi-spherical bulge component. These bulges represent an important component of the stellar mass in only 31 of the 153 SPARC galaxies. For these galaxies, we treat the bulges as spherical mass components distinct from the stellar disks. This detail only affects the the estimate of g_{bar} at the innermost points of a few galaxies with large bulges.

Stellar Mass-to-Light Ratios

We observe starlight while physics requires stellar mass. The mass-to-light ratio $\Upsilon_\star$ is thus an unavoidable conversion factor. The most robust indicator of stellar mass is the near-infrared luminosity [33].

We have constructed stellar population synthesis models of star forming disk galaxies [25] to estimate the mass-to-light ratio in the 3.6μm band of *Spitzer*. The numerical value of $\Upsilon_\star^{[3.6]}$ depends only weakly on age and metallicity for a broad range of models with different star formation histories. Here we adopt $\Upsilon_\star^{[3.6]} = 0.50$ M$_\odot$/L$_\odot$ [25] as representative of all disks of all morphological types. Independent estimates range from 0.42 M$_\odot$/L$_\odot$ [26] to 0.60 M$_\odot$/L$_\odot$ [24]. By astronomical standards, this is a small systematic uncertainty, which we explore
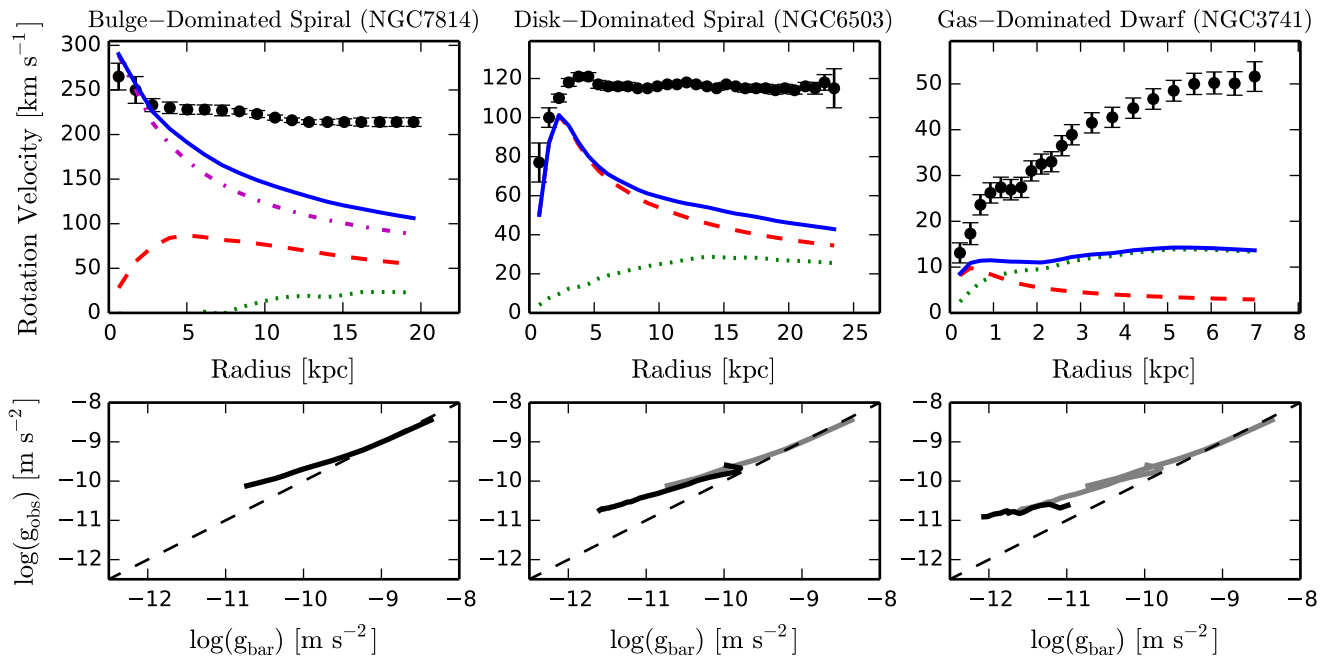
FIG. 2. Examples of mass models and rotation curves for individual galaxies. The points with error bars in the upper panels are the observed rotation curves $V(R)$. The errors represent both random errors and systematic uncertainty in the circular velocity due to asymmetry in the velocity field. In all galaxies, the data exceed the lines $v_{\rm bar} = \sqrt{Rg_{\rm bar}}$ representing the baryonic mass models (eq. 3), indicating the need for dark matter. Each baryonic component is represented: dotted lines for the gas, dashed lines for the stellar disk, and dash-dotted lines for the bulge, when present. The sum of these components is the baryonic mass model (solid line). The lower panels illustrate the run of $g_{\rm bar}$ and $g_{\rm obs}$ for each galaxy, with the dashed line being the line of unity. Note that higher accelerations occur at smaller radii. From left to right each line is replotted in gray to illustrate how progressively fainter galaxies probe progressively lower regimes of acceleration.

in a companion paper [34]. Adopting different $\Upsilon_\star$ only affects details, not the basic result.

The use of a single mass-to-light ratio is a great advance over previous work. Rather than treat $\Upsilon_\star$ as an adjustable parameter for each and every galaxy [14], it is fixed to a single value for all disks. While there is surely some scatter about the central value, adopting a universal $\Upsilon_\star$ provides a direct representation of the data with an absolute minimum of assumptions. It essentially just places the stars and gas on the same scale. The basic result follows simply from the luminosity profiles of each component.

We make one small concession to astronomical complexity. While population synthesis models predict very similar $\Upsilon_\star$ for all star forming disks, they anticipate higher $\Upsilon_\star$ for the old stars of central bulges. Hence we adopt $\Upsilon_\star^{[3.6]} = 0.7~{\rm M_\odot/L_\odot}$ for bulges [25]. This two-component population model only applies to the 31 of 153 galaxies with bulges, and has only a small effect on the estimate of $g_{\rm bar}$ in the innermost regions where the bulge dominates (Fig. 2).

RESULTS

The mass models of individual galaxies are quite diverse (Fig. 2). Bright, high surface brightness galaxies have stellar components that make a substantial contribution to the mass at small radii. Indeed, it is common for these objects to approach the regime of "maximum disk" [35]. Stars suffice to explain most of the observed rotation at small radii (Fig. 2). At the opposite extreme, the mass discrepancy is large ($V \gg V_{\rm bar}$) in low surface brightness galaxies. These require lots of dark matter, even at small radii [9, 36]. Nevertheless, the observed acceleration $g_{\rm obs}$ correlates strongly with that predicted by the baryons $g_{\rm bar}$ for all galaxies (Fig. 3).

The correlation between $g_{\rm obs}$ and $g_{\rm bar}$ in Fig. 3 refers to the observed and expected centripetal acceleration. Initially, this radial acceleration relation might seem trivial: acceleration correlates with acceleration. However, the axes of Fig. 3 are completely independent. The ordinate, $g_{\rm obs}$, is obtained from the rotation curves. The abscissa, $g_{\rm bar}$, is obtained from the observed distribution of baryons via the Poisson equation. There is no guarantee that $g_{\rm obs}$ should correlate with $g_{\rm bar}$ when dark matter dominates.
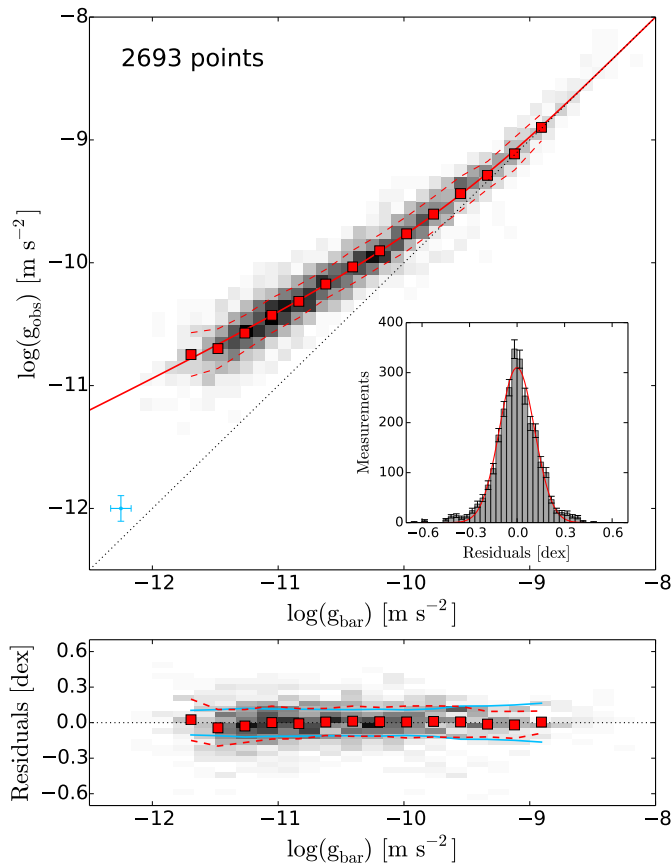
TABLE I. Scatter Budget for Acceleration Residuals

Source	Residual
Rotation velocity errors	0.03 dex
Disk inclination errors	0.05 dex
Galaxy distance errors	0.08 dex
Variation in mass-to-light ratios	0.06 dex
HI flux calibration errors	0.01 dex
Total	0.12 dex

Figure 3 combines and generalizes four well-established properties of rotating galaxies: flat rotation curves in the outer parts of spiral galaxies [1, 2]; the "conspiracy" that spiral rotation curves show no indication of the transition from the baryon-dominated inner regions to the outer parts that are dark matter-dominated in the standard model [35]; the Tully-Fisher [3] relation between the outer velocity and the inner stellar mass, later generalized to the stellar plus atomic hydrogen mass [4]; and the relation between the central surface brightness of galaxies and their inner rotation curve gradient [37–39].

It is convenient to fit a function that describes the data. The function [40]

$$g_{\rm obs} = \mathcal{F}(g_{\rm bar}) = \frac{g_{\rm bar}}{1 - e^{-\sqrt{g_{\rm bar}/g_\dagger}}} \tag{4}$$

provides a good fit. The one fit parameter is the acceleration scale, $g_\dagger$, where the mass discrepancy becomes pronounced. For our adopted $\Upsilon_\star$, we find $g_\dagger = 1.20 \pm 0.02$ (random) ± 0.24 (systematic) $\times 10^{-10}$ m s^{-2}. The random error is a 1σ value, while the systematic uncertainty represents the 20% normalization uncertainty in $\Upsilon_\star$.

Equation 4 provides a good description of $\sim$2700 individual data points in 153 different galaxies. This is a rather minimalistic parameterization. In addition to the scale $g_\dagger$, eq. 4 implicitly contains a linear slope at high accelerations and $g_{\rm obs} \propto \sqrt{g_{\rm bar}}$ at low accelerations. The high end slope is sensible: dark matter becomes negligible at some point. The low end slope of the data could in principle differ from that implicitly assumed by eq. 4, but if so there is no indication in these data.

Residuals from the fit are well described by a Gaussian of width 0.11 dex (Fig. 3). The rms scatter is 0.13 dex owing to the inevitable outliers. These are tiny numbers by the standards of extragalactic astronomy. The intrinsic scatter in the relation must be smaller still once scatter due to errors are accounted for.

There are two types of extrinsic scatter in the radial acceleration relation: measurement uncertainties and galaxy to galaxy variation in $\Upsilon_\star$. Measurement uncertainties in $g_{\rm obs}$ follow from the error in the rotation velocities, disk inclinations, and galaxy distances. The mean contribution of each is given in Table I. Intrinsic scatter about the mean mass-to-light ratio is anticipated to be

FIG. 3. The centripetal acceleration observed in rotation curves, $g_{\rm obs} = V^2/R$, is plotted against that predicted for the observed distribution of baryons, $g_{\rm bar} = |\partial\Phi_{\rm bar}/\partial R|$ in the upper panel. Nearly 2700 individual data points for 153 SPARC galaxies are shown in grayscale. The mean uncertainty on individual points is illustrated in the lower left corner. Large squares show the mean of binned data. Dashed lines show the width of the ridge as measured by the rms in each bin. The dotted line is the line of unity. The solid line is the fit of eq. 4 to the unbinned data using an orthogonal-distance-regression algorithm that considers errors on both variables. The inset shows the histogram of all residuals and a Gaussian of width $\sigma = 0.11$ dex. The residuals are shown as a function of $g_{\rm obs}$ in the lower panel. The error bars on the binned data are smaller than the size of the points. The solid lines show the scatter expected from observational uncertainties and galaxy to galaxy variation in the stellar mass-to-light ratio. This extrinsic scatter closely follows the observed rms scatter (dashed lines): the data are consistent with negligible intrinsic scatter.

Nevertheless, the radial acceleration relation persists for all galaxies of all types. Some galaxies only probe the high acceleration regime while others only probe the low end (Fig. 2). The outer regions of high surface brightness galaxies map smoothly to the inner regions of low surface brightness galaxies. These very different objects evince the same mass discrepancy at the same acceleration. Individual galaxies are indistinguishable in Fig. 3.

0.11 dex at 3.6μm [24]. This propagates to a net residual of 0.06 dex in g_{bar} after accounting for the variable slope of the relation. The total expected scatter is 0.12 dex (Table I), leaving little room for intrinsic scatter.

Astronomical data often suffer from unrecognized systematics. In the case of rotation curves, this is frequently argued [41–43] to be the cause of the apparent discrepancy [44] with the predictions of numerical simulations [45]. This cannot be the case here. If we had neglected some important source of uncertainty, we would erroneously infer a large intrinsic scatter, not a small one. For the intrinsic scatter to be non-negligible, the errors must be overestimated rather than underestimated. If there were no observational uncertainty at all, the intrinsic scatter would still be limited by the small observed rms of 0.13 dex.

Regardless of whether the intrinsic scatter is zero or merely very small, the radial acceleration relation is an important empirical facet of the mass discrepancy problem. When g_{bar} is observed, g_{obs} follows, and vice-versa. This must be explained by any successful theory.

DISCUSSION

We find a strong relation between the observed radial acceleration g_{obs} and that due to the baryons, g_{bar}. This radial acceleration relation is completely empirical. It follows from a minimum of assumptions. The only inputs are the data, the Poisson equation, and the simplest possible conversion of starlight to stellar mass.

We have not considered any particular halo model for the dark matter. Indeed, such models are unnecessary. The distribution of dark matter follows directly from the relation, and can be written entirely in terms of the baryons:

$$g_{DM} = g_{obs} - g_{bar} = \frac{g_{bar}}{e^{\sqrt{g_{bar}/g_\dagger}} - 1}. \qquad (5)$$

The dark and baryonic mass are strongly coupled [13, 14].

Possible interpretations for the radial acceleration relation fall into three broad categories.

1. It represents the end product of galaxy formation.

2. It represents new dark sector physics that leads to the observed coupling.

3. It is the result of new dynamical laws rather than dark matter.

None of these options are entirely satisfactory.

In the standard cosmological paradigm, galaxies form within dark matter halos. Simulations of this process do not naturally lead to realistic galaxies [44, 46]. Complicated accessory effects ("feedback") must be invoked to remodel simulated galaxies into something more akin to observations. Whether such processes can satisfactorily explain the radial acceleration relation and its small scatter remains to be demonstrated [47, 48].

Another possibility is new "dark sector" physics. The dark matter needs to respond to the distribution of baryons (or vice-versa) in order to give the observed relation. This is not trivial to achieve, but the observed phenomenology might emerge if dark matter behaves as a fluid [49, 50] or is subject to gravitational polarization [51].

Thirdly, the one-to-one correspondence between g_{bar} and g_{obs} suggests that the baryons are the source of the gravitational potential. In this case, one might alter the laws of dynamics rather than invoke dark matter. Indeed, our results were anticipated over three decades ago by MOND [52]. Whether this is a situation in which it would be necessary to invent MOND if it did not already exist is worthy of contemplation.

In MOND, eq. 4 is related to the MOND interpolation function. However, we should be careful not to confuse data with theory. Equation 4 provides a convenient description of the data irrespective of MOND.

Regardless of its theoretical basis, the radial acceleration relation exists as an empirical relation. The acceleration scale $g_\dagger$ is in the data. The observed coupling between g_{obs} and g_{bar} demands a satisfactory explanation. The radial acceleration relation appears to be a law of nature, a sort of Kepler's law for rotating galaxies.

[1] V. C. Rubin, N. Thonnard, and W. K. Ford, Jr., Astrophys. J. **225**, L107 (1978).
[2] A. Bosma, Astron. J. **86**, 1791 (1981).
[3] R. B. Tully and J. R. Fisher, Astron. Astrophys. **54**, 661 (1977).
[4] S. S. McGaugh, J. M. Schombert, G. D. Bothun, and W. J. G. de Blok, Astrophys. J. **533**, L99 (2000).

[5] M. A. W. Verheijen, Astrophys. J. **563**, 694 (2001).

[6] S. Courteau and H. Rix, Astrophys. J. **513**, 561 (1999).

[7] S. S. McGaugh, Phys. Rev. Lett. **95**, 171302 (2005).

[8] M. A. Zwaan, J. M. van der Hulst, W. J. G. de Blok, and S. S. McGaugh, Mon. Not. R. Astron. Soc. **273**, L35 (1995).

[9] S. S. McGaugh and W. J. G. de Blok, Astrophys. J. **499**, 41 (1998).

[10] S. S. McGaugh, Physical Review Letters **106**, 121303 (2011), arXiv:1102.3913 [astro-ph.CO].

[11] S. S. McGaugh and J. M. Schombert, Astrophys. J. **802**, 18 (2015), arXiv:1501.06826.

[12] F. Lelli, S. S. McGaugh, and J. M. Schombert, Astrophys. J. **816**, L14 (2016), arXiv:1512.04543.

[13] R. Sancisi, in *Dark Matter in Galaxies*, IAU Symposium, Vol. 220, edited by S. Ryder, D. Pisano, M. Walker, and K. Freeman (2004) p. 233, arXiv:astro-ph/0311348.

[14] S. S. McGaugh, Astrophys. J. **609**, 652 (2004).

[15] S. S. McGaugh, Galaxies **2**, 601 (2014), arXiv:1412.3767.

[16] R. Scarpa, in *First Crisis in Cosmology Conference*, American Institute of Physics Conference Series, Vol. 822, edited by E. J. Lerner and J. B. Almeida (2006) pp. 253–265, astro-ph/0601478.

[17] M. den Heijer, T. A. Oosterloo, P. Serra, G. I. G. Józsa, J. Kerp, R. Morganti, M. Cappellari, T. A. Davis, P.-A. Duc, E. Emsellem, D. Krajnović, R. M. McDermid, T. Naab, A.-M. Weijmans, and P. T. de Zeeuw, Astron. Astrophys. **581**, A98 (2015), arXiv:1509.05236.

[18] P. Serra, T. Oosterloo, M. Cappellari, M. den Heijer, and G. I. G. Józsa, Mon. Not. Royal Astron. Soc. (2016), 10.1093/mnras/stw1010.

[19] F. Lelli, S. S. McGaugh, and J. M. Schombert, Astron. J. (2016), arXiv:1606.09251.

[20] R. Lange, S. P. Driver, A. S. G. Robotham, L. S. Kelvin, A. W. Graham, M. Alpaslan, S. K. Andrews, I. K. Baldry, S. Bamford, J. Bland-Hawthorn, S. Brough, M. E. Cluver, C. J. Conselice, L. J. M. Davies, B. Haeussler, I. S. Konstantopoulos, J. Loveday, A. J. Moffett, P. Norberg, S. Phillipps, E. N. Taylor, Á. R. López-Sánchez, and S. M. Wilkins, Mon. Not. Royal Astron. Soc. **447**, 2603 (2015), arXiv:1411.6355.

[21] J. D. Bradford, M. C. Geha, and M. R. Blanton, Astrophys. J. **809**, 146 (2015), arXiv:1505.04819.

[22] K. D. Eckert, S. J. Kannappan, D. V. Stark, A. J. Moffett, A. A. Berlind, and M. A. Norris, Astrophys. J. **824**, 124 (2016), arXiv:1604.03957.

[23] J. M. Schombert and S. McGaugh, Pub. Astron. Soc. Australia **31**, e011 (2014), arXiv:1401.0238.

[24] S. E. Meidt, E. Schinnerer, G. van de Ven, D. Zaritsky, R. Peletier, J. H. Knapen, K. Sheth, M. Regan, M. Querejeta, J.-C. Muñoz-Mateos, T. Kim, J. L. Hinz, A. Gil de Paz, E. Athanassoula, A. Bosma, R. J. Buta, M. Cisternas, L. C. Ho, B. Holwerda, R. Skibba, E. Laurikainen, H. Salo, D. A. Gadotti, J. Laine, S. Erroz-Ferrer, S. Comerón, K. Menéndez-Delmestre, M. Seibert, and T. Mizusawa, Astrophys. J. **788**, 144 (2014), arXiv:1402.5210.

[25] J. Schombert and S. McGaugh, Pub. Astron. Soc. Australia **31**, e036 (2014), arXiv:1407.6778.

[26] S. S. McGaugh and J. M. Schombert, Astron. J. **148**, 77 (2014), arXiv:1407.1839.

[27] T. P. K. Martinsson, M. A. W. Verheijen, K. B. Westfall, M. A. Bershady, D. R. Andersen, and R. A. Swaters, Astron. Astrophys. **557**, A131 (2013), arXiv:1308.0336 [astro-ph.CO].

[28] B. T. Draine, *Physics of the Interstellar and Intergalactic Medium* (Princeton, NJ, Princeton University Press, 2011).

[29] E. Aver, K. A. Olive, and E. D. Skillman, JCAP **5**, 003 (2010), arXiv:1001.5218.

[30] S. Casertano, Mon. Not. Royal Astron. Soc. **203**, 735 (1983).

[31] J. Binney and S. Tremaine, *Galactic Dynamics* (Princeton, NJ, Princeton University Press, 1987).

[32] J. M. van der Hulst, J. P. Terlouw, K. G. Begeman, W. Zwitser, and P. R. Roelfsema, in *Astronomical Data Analysis Software and Systems I*, Astronomical Society of the Pacific Conference Series, Vol. 25, edited by D. M. Worrall, C. Biemesderfer, and J. Barnes (1992) p. 131.

[33] E. F. Bell and R. S. de Jong, Astrophys. J. **550**, 212 (2001).

[34] F. Lelli, S. S. McGaugh, and J. M. Schombert, Astrophys. J. , in prep. (2016).

[35] T. S. van Albada and R. Sancisi, Philosophical Transactions of the Royal Society of London Series A **320**, 447 (1986).

[36] W. J. G. de Blok and S. S. McGaugh, Mon. Not. Royal Astron. Soc. **290**, 533 (1997), astro-ph/9704274.

[37] W. J. G. de Blok and S. S. McGaugh, Astrophys. J.l **469**, L89 (1996), astro-ph/9607042.

[38] F. Lelli, F. Fraternali, and M. Verheijen, Mon. Not. Royal Astron. Soc. **433**, L30 (2013), arXiv:1304.4250.

[39] F. Lelli, S. S. McGaugh, J. M. Schombert, and M. S. Pawlowski, Astrophys. J. **827**, L19 (2016), arXiv:1607.02145.

[40] S. S. McGaugh, Astrophys. J. **683**, 137 (2008), arXiv:0804.1314.

[41] F. C. van den Bosch and R. A. Swaters, Mon. Not. Royal Astron. Soc. **325**, 1017 (2001), astro-ph/0006048.

[42] K. A. Oman, J. F. Navarro, L. V. Sales, A. Fattahi, C. S. Frenk, T. Sawala, M. Schaller, and S. D. M. White, Mon. Not. Royal Astron. Soc. **460**, 3610 (2016), arXiv:1601.01026.

[43] J. C. B. Pineda, C. C. Hayward, V. Springel, and C. Mendes de Oliveira, ArXiv e-prints (2016), arXiv:1602.07690.

[44] W. J. G. de Blok, Advances in Astronomy **2010**, 789293 (2010), arXiv:0910.3538.

[45] J. F. Navarro, C. S. Frenk, and S. D. M. White, Astrophys. J. **490**, 493 (1997).

[46] S. S. McGaugh, Canadian Journal of Physics **93**, 250 (2015), arXiv:1404.7525.

[47] A. Di Cintio and F. Lelli, Mon. Not. Royal Astron. Soc. **456**, L127 (2016), arXiv:1511.06616.

[48] H. Desmond, arXiv:1607.01800 (2016), arXiv:1607.01800.

[49] H. Zhao and B. Li, Astrophys. J. **712**, 130 (2010), arXiv:0804.1588.

[50] J. Khoury, Phys. Rev. D **91**, 024022 (2015), arXiv:1409.0012 [hep-th].

[51] L. Blanchet, Classical and Quantum Gravity **24**, 3529 (2007).

[52] M. Milgrom, Astrophys. J. **270**, 371 (1983).